

## THE INFLUENCE OF TREATMENT PARAMETERS ON THE MICROSTRUCTURE, PROPERTIES AND BEND ANGLE OF LASER FORMED CONSTRUCTION BARS

In this paper, the authors presented the research on laser formed construction bars made of C20 steel on the example of the T-shape. The CO<sub>2</sub> TRUMPF TruFlow 6000 laser was used in the research. The influence of the laser treatment parameters (the power and speed of the heat source) on the volume of the bend angle, structure and properties of the elements (hardness and tensile strength) was examined. On the basis of the results obtained from the conducted experiments, the authors suggested a way of selecting treatment parameters so that the element should meet the strength assumptions at the allowable time of its implementation.

*Keywords:* Laser forming, Laser treatment, Microstructure, Fourier number

### 1. Introduction

The laser forming is a kind of laser thermal treatment technologies [1-2]. The laser forming is one of the methods of inducing the contactless tension in the material which leads to permanent plastic strain. The phenomenon of the thermal expansion is the mechanism which allows this process. It can induce the thermal expansions sufficient to obtain the permanent deformations. Therefore laser forming is one of the thermal shaping methods. In order to obtain plastic distortions, the material (mainly iron alloys) should be heated above the so-called plasticizing temperature  $T_{pl}$  [3-4]. Above this temperature, the yield point  $R_e$  and a longitudinal modulus of elasticity  $E$  decreases rapidly as shown in the Prandtl diagram Fig. 1.

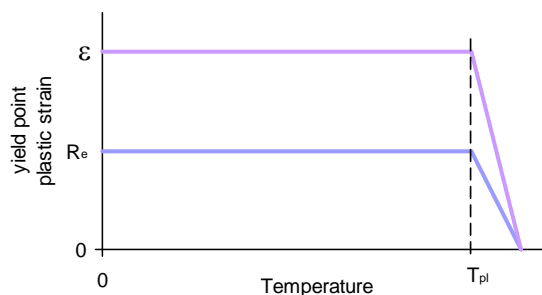


Fig. 1. Prandtl diagram [3]

This temperature for steel is approximately 870°K. It means that in order to make a permanent thermal deformation in the material, it must be heated above the  $T_{pl}$  temperature. However,

in order to avoid undesirable structural changes affecting the changes in the element properties, the process temperature should not exceed approximately 1000°K (for the steel – it is the eutectoid transition temperature). At the same time, according to the equation (1) [5], the higher process temperature, the (theoretically) greater bend angle of the treated element. Consequently, to make the laser forming technology fulfill its task, it is necessary to determine such a process temperature at which the bend angle will be relatively high, and the changes in structure will not affect significantly the properties of the finished elements [6].

### 2. T-bar laser forming experiment

In order to select the parameters, T-bar laser forming experiment was prepared and performed. The course and results of the experiment have been presented in the below mentioned sub-sections.

#### 2.1. Parameters selection for the laser forming process

The process parameters were selected from the condition that the  $\alpha_b$  bend angle will be constant and will be  $\alpha_b = 0.1^\circ$ . The theoretical bend angle was calculated using a following formula [4]:

$$\alpha_b = 12 \sqrt{\frac{2}{e}} F_0 \frac{\alpha_{th} AP}{\pi \lambda d} \left\{ \ln \theta_S - \sqrt{\frac{2}{e}} F_0 [\theta_S - \ln(e \theta_S)] \right\} \quad (1)$$

\* KIELCE UNIVERSITY OF TECHNOLOGY, LASER PROCESSING RESEARCH CENTRE, 7<sup>th</sup> TYŚIĄCŁECIA P.P. AV. 25-314 KIELCE, POLAND

# Corresponding author: pkurp@tu.kielce.pl

Where:  $\theta_s$  is a dimensionless surface temperature expressed by the equation:

$$\theta_s = \frac{4AP}{\pi\lambda\Delta T_{pl}} \sqrt{\frac{\kappa}{vd^3}} \quad (2)$$

While  $F_0$  is the Fourier number expressed by the equation:

$$F_0 = \frac{\kappa d}{vg^2} \quad (3)$$

The data and parameters used for the calculations were as follows:

Material constants:  $\alpha_{th} = 1.3 \times 10^{-6} \text{ 1/}^\circ\text{K}$  – thermal expansion coefficient;  $\kappa = 1.13 \times 10^{-5} \text{ m}^2/\text{s}$  – thermal diffusivity;  $\lambda = 40 \text{ W/mK}$  – thermal conductivity coefficient.

Processing parameters:  $A = 0.6$  – surface absorption coefficient;  $d = 2.5 \text{ mm}$  – the diameter of the laser beam on the surface of the treated element;  $P$  – laser power (depending on the speed and the desired bend angle);  $v$  – the speed of heat source (depending on the power and the desired bend angle).

On the basis of the presented at the beginning of the paragraph condition  $\alpha_b = 0,1^\circ$  and basing on the equations (1), (2) and (3), the process parameters were calculated in two variants:

$$P = 300\text{W}; v = 0,4 \text{ m/min} \rightarrow \alpha_b = 0,17^\circ \quad (a)$$

$$P = 800\text{W}; v = 3,7 \text{ m/min} \rightarrow \alpha_b = 0,16^\circ \quad (b)$$

Due to the fact that the T-bar has a central stiffening part, it affects the so-called rigidity of the element. In accordance with the above, the calculated value of the bend angle  $\alpha_b$ , should be corrected by the  $R_r = 0.65$  rigidity coefficient [6]. After correction, we obtain the value  $\alpha_b = 0.1^\circ$ . On this basis, the experiment was planned and performed.

## 2.2. Research station and conducting experiment

In order to perform the T-bar bending to have the calculated angle, the experiment was conducted with the use of CO<sub>2</sub> laser by TRUMPF, TruFlow 6000 model. The bending was made using a triangular plasticizing zone, by the laser upsetting mechanism (Fig. 2). The research position view has been shown in Fig. 3.

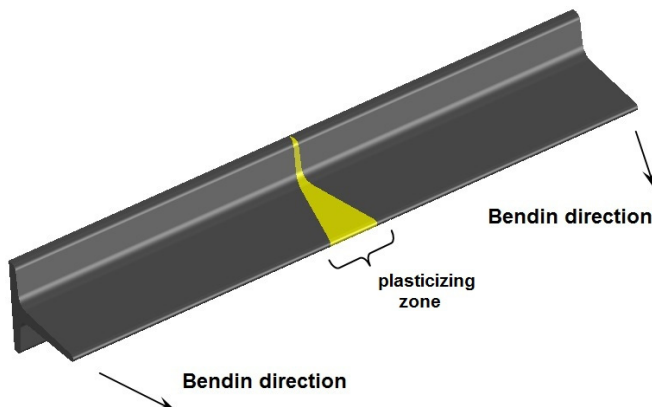


Fig. 2. Heating scheme using triangular plasticizing zone and the anticipated direction of the bend

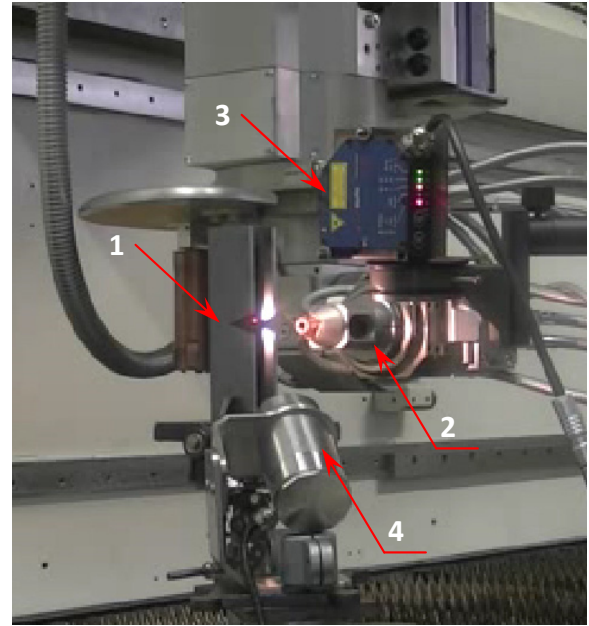


Fig. 3. TRUMPF TruFlow 6000 research position view

In order to conduct the experiment, made of C20 steel even-armed T-bar of dimensions  $25 \times 25 \times 3 \text{ mm}$  and the length of  $150 \text{ mm}$  was used. The triangular plasticizing zone was obtained by applying the proper masks **1** to the tested element, between which the sample was placed. The element was heated by a lenticular laser head **2**. The bend angle was measured by MicroEpsilon OptoNCDT 1700-1720 **3** contactless laser range-finder. During the process, the temperature of the directly heated surface was also registered (from the side of the laser head) as well as the opposite side (“cold”). For this purpose the OPRIS G5H monochromatic optical pyrometer **4** was used. The results of the experiment have been shown in the section below.

## 3. Experiment results

The experiment included:

- the measurement of the bend angle change during the treatment;
- the measurement of the temperature changes during the treatment;
- microstructure testing;
- hardness testing;
- tensile testing.

### 3.1. Bend angle measurement

The bend angle change during the process for the proposed parameters was registered in the real time using the MicroEpsilon OptoNCDT 1700-20 rangefinder laser. There were made four heating tests for each parameter presented in the section 2.1. The results of bend angle measurements have been illustrated in Fig. 4 and Fig. 5.

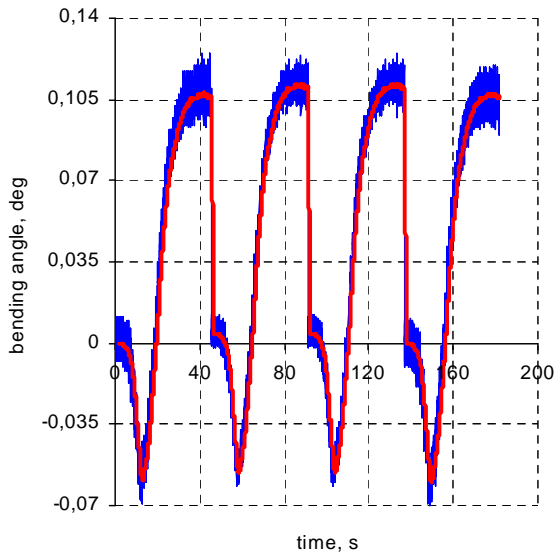


Fig. 4. The bending angle change according to (a) treatment parameters

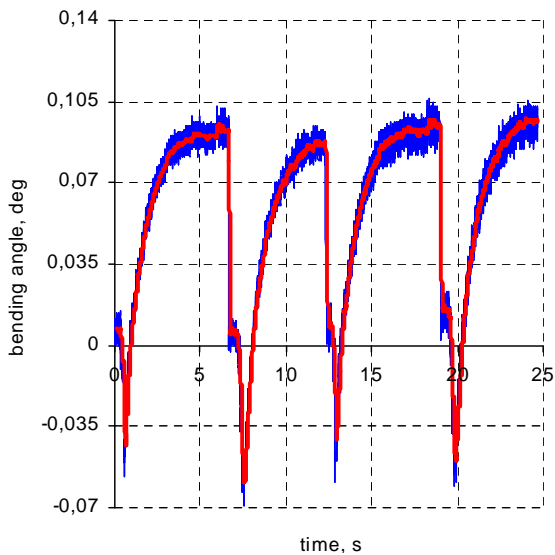


Fig. 5. The bending angle change according to (b) treatment parameters

As results from the graphs presented above, the bend angle is close to the theoretical one according to the equation (1). The initial downward peak is a result of the rigidity of the element. It appears in both cases (a) and (b). In case (b), due to the higher velocity of the process, the effect was achieved in the shorter time. However, the bend angle is approximately 10% lower for the parameters (b) in relation to the case (a). A summary of the results obtained is presented in Table 1.

TABLE 1

Bending angles obtained after laser forming

(a) treatment parameters		(b) treatment parameters	
Bending angle	Average bending angle	Bending angle	Average bending angle
0,099°	0,104°	0,098°	0,097°
0,107°		0,089°	
0,108°		0,099°	
0,101°		0,101°	

### 3.2. Temperature changes measurement

Due to the fact that laser forming is a thermal technology, the knowledge of temperature changes during the process is essential. This will allow us to determine the real isotherms during the process as well as to arrange a further discussion concerning structural changes of the processed elements. During the process, the temperature of both the surface treated directly with the laser beam (two high peaks at the graphs below) and the opposite surface (two low peaks at the graphs below) were measured. The OPRIS G5H monochromatic optical pyrometer was used in order to measure the temperature.

The course of temperature changes for processing parameters (a) and (b) has been shown in Fig. 6 and Fig. 7.

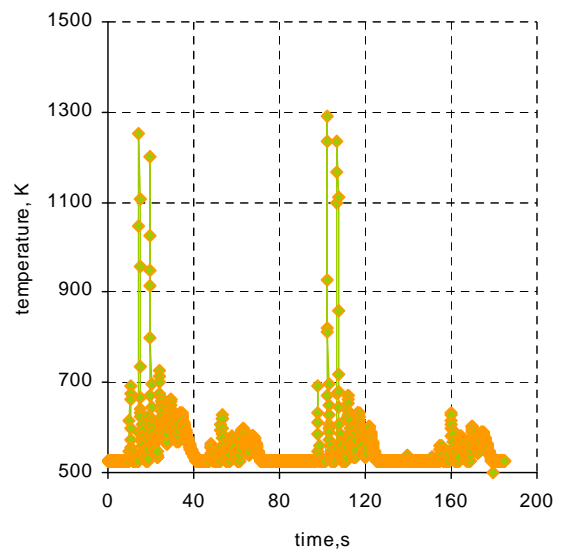


Fig. 6. Temperature changes during the process according to (a) treatment parameters

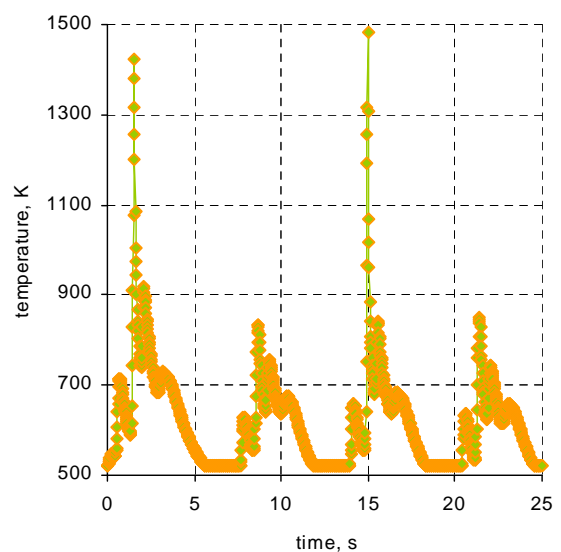


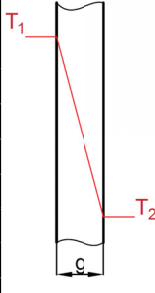
Fig. 7. Temperature changes during the process according to (b) treatment parameters

As can be seen from the graphs, the temperature differences between the surface directly heated and the parallel surface are

significant, and in both cases this difference was approximately 600°K. It means that the temperature gradient appears on the sample's thickness. The gradient values have been presented in Table 2.

TABLE 2

The temperature difference (gradient) between the directly heated surface and the opposite surface

The surface directly exposed to the laser beam		The surface parallel to directly exposed to the laser beam
$T_1$ temperature, K		$T_2$ temperature, K
(a) treatment parameters	(a) treatment parameters	
1280	660	
1300	650	
(b) treatment parameters	(b) treatment parameters	
1420	870	
1490	880	

In connection with the gradient appearance on the sample's thickness, one may expect many types of structures in the axis of laser beam operation.

### 3.3. Microstructures testing

In order to identify the microstructure in the axis of the laser beam the metallographic specimens were made. The specimens after nital etching were under microscopic observations with the use of the JEOL JSM 5400 electron microscope.

As for the processed elements, one should expect the structure change being a result of phase changes in the material, depending on temperature and exposure time. In both cases (a) and (b) the base material has a ferritic-pearlitic structure, which was shown in Fig. 8.

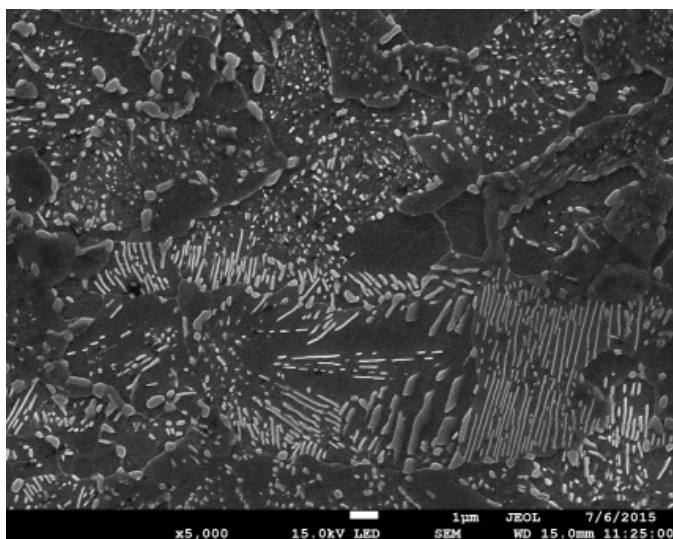


Fig. 8. The base material ferrite-pearlite structure view

In the heat affected zone the martensitic structure was created (Fig. 9). However, the HAZ extent is different in both cases. For the processing with parameters (a), the martensite can be observed up to the depth of approximately 450 µm, and with parameters (b) up to about 600 µm. Furthermore, in the case of processing with the parameters (b) under the martensite layer there is a fine-grained ferritic-pearlitic layer of about 50 µm thick (Fig. 10), and on the surface directly operated by a laser beam there is an oxide layer of about 20 µm thick (Fig. 11). In the element made with the parameters (a), none of the described changes were observed.

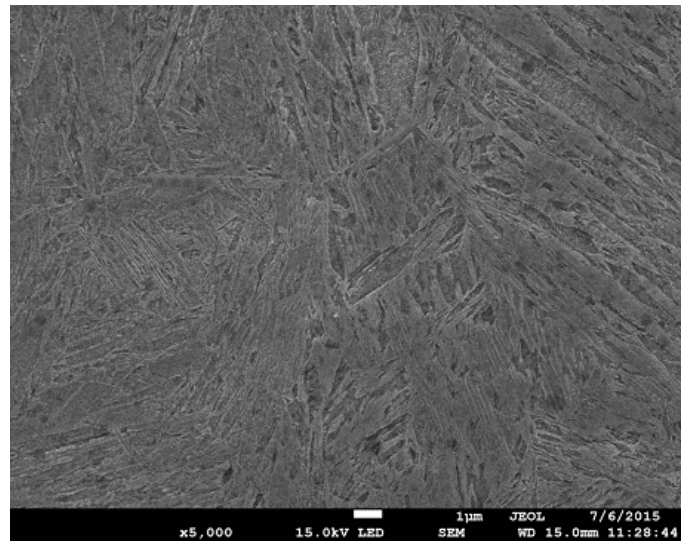


Fig. 9. HAZ martensitic structure view

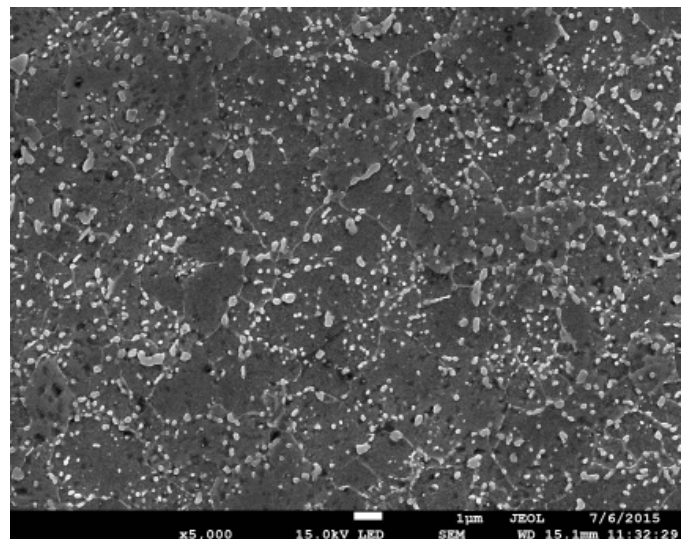


Fig. 10. HAZ fine ferrite-pearlite structure view

Since structure changes have an influence on the mechanical properties of made elements, their hardness and tensile was tested.

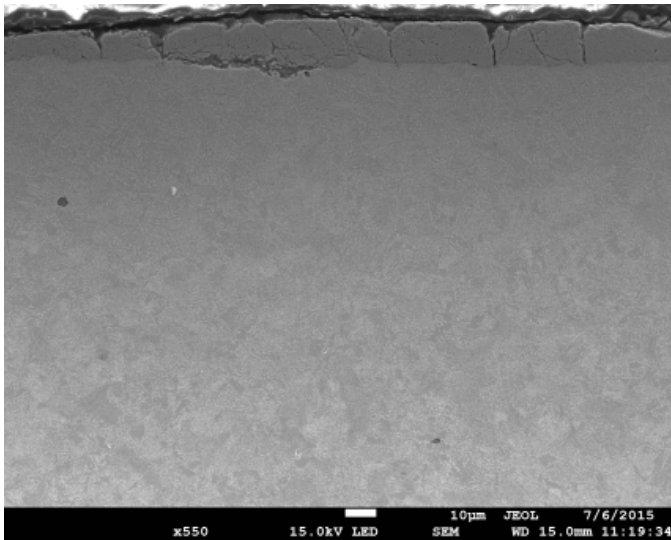


Fig. 11. View of the oxide layer formed on the specimen's surface treated with (b) parameters

### 3.4. Hardness testing

In order to check the influence of the laser processing parameters on the material properties, the surface hardness measurement was made using the Vickers's method. The measurement was made using the Nexus InnovaTest 4303D hardness tester. The hardness measurement of the element in the axis of laser beam operation was conducted several times. The measurement was performed at the load of 0.1 kG at distances of 0.02 mm. The results have been shown in Fig. 12 and Fig. 13.

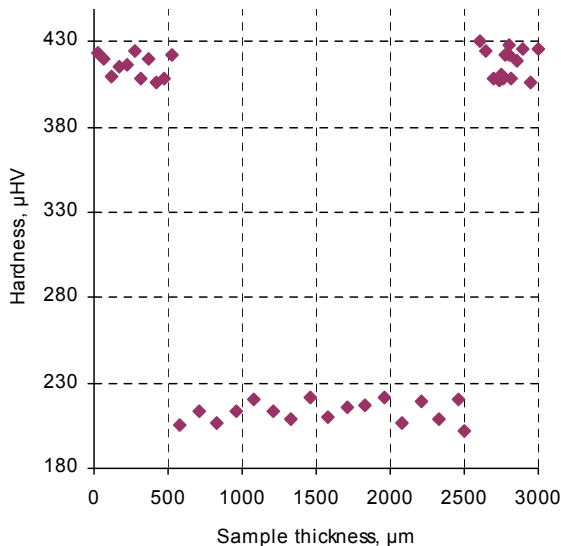


Fig. 12. Hardness differences thru the thickness of the specimen treated with (a) parameters

As results from the presented graphs, the hardness of each created layers significantly differs. For the bended sample with the (a) parameters there can be clearly seen a distinction between the hard martensite zone of about 430 HV and the zone of soft

base material of about 230 HV. On the other hand, in the case of the bended specimen with the (b) parameters, the change of the hardness presents as following: oxide layer approx. 480 HV, martensitic structure approx. 440 HV, fine-grained ferrite-pearlite structure approx. 330 HV, ferrite-pearlite base material approx. 220 HV. Therefore the separate mechanic properties can be expected for each presented case. In the mentioned below subsection, the tensile strength of the specimens was tested.

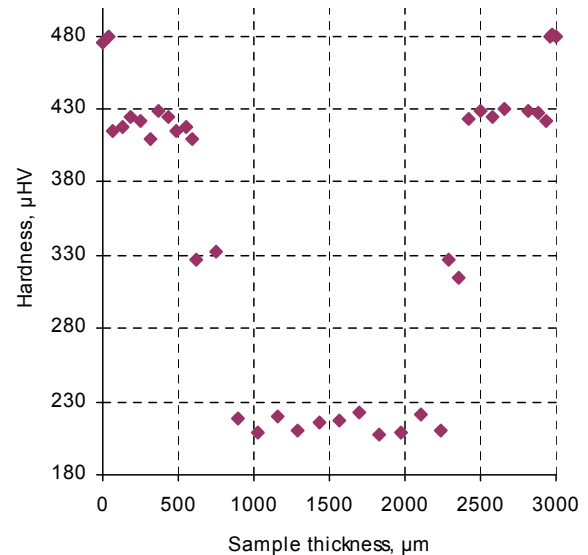


Fig. 13. Hardness differences thru the thickness of the specimen treated with (b) parameters

### 3.5. Tensile strength testing

Changes in the structure during the thermal processing have an influence also on the change in the yield strength and tensile strength. To identify those steel properties after (a) and (b) parameters treatment, the tests using the Instron model 8501 tensile testing machine were conducted. The test was conducted basing on the PN-H-04310:1991, PN-EN 10002-1:2004 standards [7,8]. Samples were made of the C20 flat steel sheet, previously treated by the two-sided laser scanning. Scanning parameters were identical to the parameters used in the laser forming. A specimen made of a normalized steel sheet, not treated by any processing, was used as a control one. Results of the static tensile test have been summarized in Fig. 14.

Both for the normalized steel specimen and for the treated one with the parameters (a) the yield strength can be clearly seen. In the case of the sample treated with parameters (b), the clear yield limit cannot be observed. The tensile strength is the highest for the specimen processed with the (b) parameters and is approx.  $R_m = 800$  MPa in comparison to the specimen processed with the (a) parameters – approx.  $R_m = 680$  MPa and the normalized one  $R_m = 580$  MPa. At the same time, the value of the specimen elongation decreases. The specimen made with (b) parameters is the least plastic. The results obtained are a consequence of the structure created during the process of laser forming.

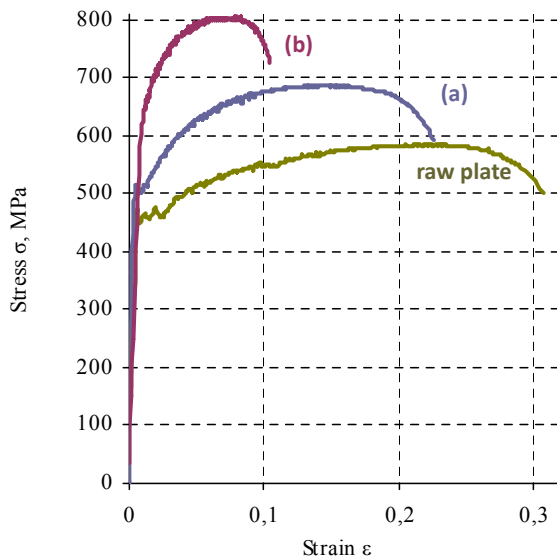


Fig. 14. The yield point and the limit of tensile strength differences depending on the treatment parameters and the obtained structure

#### 4. Discussion concerning results

As results from the conducted tests, the obtained structure differs in relation to the used parameters of the laser processing. For the specimen made according to the (a) parameters, the HAZ structure is martensitic. While in case of the (b) parameters, the HAZ structure is more complex. In this case, also the HAZ range is deeper. This has a significant influence on the properties of the finished element, such as hardness and tensile strength.

The differences in the obtained structures, and consequently in properties, can be due to the interaction time of the heat source with the surface of the processed material. Heat is transferred into the material by diffusion. This process needs time to heat the element homogeneously. It can be illustrated using the Fourier number (3). It describes the heat diffusion velocity into the material, depending on, among others, parameters of the heat source. In the case of the element made with the (a) parameters,  $F_0 = 0.5$ , while with the (b) parameters  $F_0 = 0.05$ . Thus the difference is tenfold. It should be interpreted basing on the character of the Fourier number. It describes the heat stream conducted through the body in relation to its internal thermal energy accumulated during the heat source impact on this body. Thus, in the case of (a), the time of flow of the heat through the body (mainly through its thickness) is so high that the element heats evenly and cools evenly. However, in the case of (b), the element surface heats suddenly, causing its melting and sudden cooling. Heat is transferred to the cool part of the material. Rapidly absorbed heat from the surface leads to its structural changes. This also leads to significant changes in the mechanical properties of the obtained element.

As it was mentioned in the introduction, the element should be heated at the temperatures ranging from 870°K to 1000°K. Such a temperature range would allow the sufficient material plasticity, avoiding, at the same time, phase transitions. In fact, the element surface temperature reached the temperature of

about 1500°K. It should be noted that the experiment was not performed in the laboratory conditions, but on the typically industrial laser. Therefore, it was not possible to heat the element homogeneously on its entire thickness. It was assumed that the temperature approx. 1000°K will be reached in the half of the element thickness. The result of this compromise is the fact that one surface of the sample was overheated and the other one was underheated. According to the above, the structure at the sample thickness is not uniform.

#### 5. Conclusions

Using the analytical method for calculating the bend angle for laser forming using the equation (1), it can be concluded that the selection of parameters does not affect the value of the bend angle. In both cases, the calculated bend angle (after having taken into account the rigidity coefficient  $R_r = 0.65$ ) is approx.  $\alpha_b = 0.1^\circ$ . The selection of parameters, however, is important for the properties of the obtained element. It can be stated that the sample made in accordance with the (b) parameters has a lower plasticity. It is also characterized by an increased hardness. The application of the element made with the (b) parameters in the real structure (for example the load-bearing lattice) could damage it because of poorer possibilities of its operation (poorer plasticity properties). On the other hand, a disadvantage of production of the element in accordance with the (a) parameters is four times longer production time than in the case of using the (b) parameters.

#### REFERENCES

- [1] M. Rozmus-Górnikowska, J. Kusinski, M. Blicharski, The influence of the laser treatment on microstructure of the surface layer of an X5CRNI18-10 austenitic stainless steel, *Archives of Metallurgy and Materials* **56**(3), 717-721 (2011).
- [2] A. Bartkowska, A. Pertek, M. Jankowiak, K. Józwiak, Laser surface modification of borochromizing C45 steel, *Archives of Metallurgy and Materials* **57**(1), 711-714 (2011).
- [3] M. Myśliwiec, *Ciepłno-mechaniczne podstawy spawalnictwa*, WNT, Warszawa, 1970.
- [4] Z. Mucha, J. Zajac, L. Gregova, Deformations in samples caused by irradiation of laser beam pulse CO<sub>2</sub>, *Applied Physics Letters*, (2007).
- [5] Z. Mucha, Analytical modeling of laser plates bending by use of temperature gradient and buckling mechanisms and their experimental verification, *LANE* (2007).
- [6] P. Kurp, *Modelowanie i doświadczalne badania laserowego gięcia i prostowania kształtowników konstrukcyjnych*, Rozprawa doktorska, Politechnika Świętokrzyska, Kielce, (2014).
- [7] Polska Norma PN-EN 10002-1:2004, *Metale. Próba rozciągania. Część 1: Metoda badania w temperaturze otoczenia*, (2004).
- [8] Polska Norma PN-H-04310:1991, *Próba statyczna rozciągania metali*, (1991).